

Antia, a natural anti-oxidant product, attenuates cognitive dysfunction in streptozotocin-induced mouse model of sporadic Alzheimer's disease by targeting the amyloidogenic, inflammatory, autophagy and oxidative stress pathways

Nesrine S. El Sayed¹ and Mamdooh H. Ghoneum²

¹Department of Toxicology and Pharmacology, Cairo University, Cairo, Egypt.

²Department of Surgery, Drew University of Medicine and Science, Los Angeles, California, U.S.A.

Corresponding Author: Dr. Mamdooh Ghoneum, Department of Surgery, Charles R. Drew University of Medicine and Science, 1621 E. 120th Street, Los Angeles, CA 90059, USA;
Phone: 310.474.6724; Fax: 310.474.6724; Email: mghoneum@ucla.edu

Word count: 4831

Number of Figures: 6

Number of Tables: 0

Supplementary data: n/a

Running title: Antia attenuates SAD in mice

Abstract

1
2
3
4
5
6
7
8
9
10
11
12
13
14
15
16
17
18
19
20
21
22

Background: Many neurodegenerative diseases such as Alzheimer's disease are associated with oxidative stress. Therefore, antioxidant therapy has been suggested for the prevention and treatment of neurodegenerative diseases.

Objective: We investigated the ability of the anti-oxidant Antia to exert a protective effect against sporadic Alzheimer's disease (SAD) induced in mice. Antia is a natural product that is extracted from the edible yamabushitake mushroom, the gotsukora and kothala himbutu plants, diosgenin (an extract from wild yam tubers), and amla (Indian gooseberry) after treatment with MRN-100 (an iron-based fluid).

Methods: Single intracerebroventricular (ICV) injection of streptozotocin (STZ) (3mg/kg) was used for induction of SAD in mice. Antia was injected intraperitoneally (IP) in 3 doses (25, 50 and 100 mg/kg/day) for 21 days. Neurobehavioral tests were carried out within 24h after the last day of injection. Afterwards, mice were sacrificed by cervical dislocation and decapitation. The hippocampi were rapidly excised, weighed, and homogenized to be used for measuring biochemical parameters.

Results: Treatment with Antia significantly improved mice performance on the Morris water maze. In addition, biochemical analysis showed that Antia exerted a protective effect for several compounds, including GSH, MDA, NF- κ B, IL-6, TNF- α , and amyloid- β . Further studies with Western blot showed the protective effect of Antia for the JAK2/STAT3 pathway.

Conclusions: Antia exerts a significant protection against cognitive dysfunction induced by ICV-STZ injection. This effect is achieved through targeting of the amyloidogenic, inflammatory, and

23 oxidative stress pathways. The JAK2/STAT3 pathway plays a protective role for
24 neuroinflammatory and neurodegenerative diseases such as SAD.

25

26 Key words: Alzheimer's disease, autophagy, oxidative stress, Antia, amyloid- β

27

Introduction

28

29 Age-related neurological disorders such as Alzheimer's disease (AD) are on the rise. AD
30 is a neurodegenerative disorder characterized by a progressive decline of memory and cognition,
31 and it is the most common cause of dementia, accounting for 60-80% of all cases (1). The most
32 common type of AD in the elderly, sporadic Alzheimer's disease (SAD), is associated with
33 progressive neurodegeneration of the central nervous system (2). Several pathways have been
34 examined as possible targets for SAD, including the oxidative stress, amyloidogenic, inflammatory,
35 and autophagy pathways.

36 The appearance of oxidative stress markers is one of the earliest changes in AD brains,
37 preceding the accumulation of visible amyloid deposits and neurofibrillary tangles (3). Oxidative
38 stress is implicated in many disorders like chronic inflammation, AD, and Parkinson's disease (4).
39 Neurons in the brain are at extremely high risk of excessive generation of reactive oxygen species
40 (ROS) and oxidative damage since they show high oxygen consumption and energy production
41 (5).

42 In AD brains, normally solid amyloid- β ($A\beta$) and tau proteins assemble into amyloid-like
43 filaments called plaques and tangles. It is currently unresolved how $A\beta$ accumulates in the central
44 nervous system and initiates cell disease, but a suggested mechanism by which $A\beta$ may damage
45 neurons and cause neuronal death includes ROS generation during $A\beta$ self-aggregation. When this
46 occurs on the membrane of neurons in vitro, it ultimately leads to depolarization of the synaptic
47 membrane, excessive calcium influx, and mitochondrial impairment (6-7).

48 Neurodegenerative diseases such as AD are also accompanied by neuroinflammation. The
49 transcription factor NF- κ B has been found to play a crucial role in the inflammatory response of

50 neurons. Under normal physiological conditions, NF- κ B forms a cytoplasmic complex with its
51 inhibitor I κ B α as an inactive form, but when stimulated, NF- κ B can induce the transcription of
52 inflammatory target genes such as cyclooxygenase-2 (COX-2), interleukin-1 β (IL-1 β), interleukin-
53 6 (IL-6), and tumor necrosis factor- α (TNF- α). In addition, neuroinflammation has been linked
54 with autophagy in neurodegenerative diseases. Pathological disruption of autophagy can cause an
55 initiation or exacerbation of neuroinflammation and, conversely, neuroinflammation can induce
56 an autophagic deficit that exacerbates neurodegeneration (8). In human AD, as well as in mouse
57 models of AD, autophagy has been found to be decreased and to contribute to the pathological
58 accumulation of tau aggregates (9). Autophagy is known to be regulated by mTOR, the
59 mammalian target of rapamycin, and mTOR inhibition has been shown to prevent
60 neuroinflammation in a mouse model of cerebral palsy (10). Moreover, it has been demonstrated
61 that GSK-3 β inhibition suppresses neuroinflammation in the cortices of rats subjected to ischemic
62 brain injury by activating autophagy (11).

63 Pharmacological management of AD has been limited to date. Long-term usage of non-
64 steroidal anti-inflammatory drugs (NSAIDs) were thought in 2007 to be associated with a reduced
65 likelihood of developing AD (12). Evidence also suggested the notion that NSAIDs could reduce
66 inflammation related to amyloid plaques, but trials were suspended due to high adverse events (13).
67 There are no medications or supplements that have been shown to decrease risk of AD (13), and
68 unfortunately, current FDA-approved AD treatments only offer symptomatic relief and are unable
69 to delay or cure the disease (1).

70 Recently, antioxidants have received increased attention in preventing the onset of AD by
71 reducing oxidative stress insult (14-15). Furthermore, the use of and search for drugs and dietary
72 supplements from plants have accelerated in recent years, due in part to the health benefits that

73 have been found in phytochemicals whose uses have been documented in traditional medicine (16).
74 Components of the traditional Chinese medicinal mushroom called yamabushitake promote nerve
75 growth factor synthesis in cultured astrocytes (17-18) as well as improving mild cognitive
76 impairment in humans (19). The gotsukora plant has traditionally been used for dementia and
77 memory improvement (20-21), and its extracts have been shown to improve memory retention in
78 rodents (22), alter amyloid beta pathology in the hippocampus of a mouse model of AD, and
79 modulate the oxidative stress response implicated in neurodegenerative changes that occur with
80 AD (23). Diosgenin, a plant-derived steroidal sapogenin, has been shown to exert anti-cancer
81 effects (24), improve aging-related cognitive deficits (25), and relieve diabetic neuropathy (26).
82 Recently, it was proven that diosgenin improves memory function and reduces axonal
83 degeneration in AD mouse models (20,27). Amla, the Indian gooseberry, has been shown to have
84 potent radical scavenging effects (28); to have a high degree of neuro-protective potential in a
85 panel of bioassays that targeted oxidative stress, carbonyl stress, protein glycation, A β fibrillation,
86 acetylcholinesterase inhibition, and neuroinflammation (29); and to improve the cognitive
87 functions, brain antioxidant enzymes, and acetylcholinesterase activity in a rat model of AD (30).
88 Finally, kothala himbutu (*Salacia reticulata*) has been shown to protect against deleterious
89 cognitive changes in streptozotocin-induced young diabetic rats (31) and against mercury toxicity
90 in mice hippocampi (32).

91 In this study, we examine the cogno-protective effects of an anti-oxidant product called
92 Antia whose components include yamabushitake, gotsukora, diosgenin, amla, and kothala himbutu.
93 These components are treated together with the hydroferrate fluid MRN-100 to generate Antia.
94 Previous research on MRN-100 has shown it to protect against age-associated oxidative stress (33)
95 and against oxidative damage in endothelial cells as well as in murine and human leukemia cells

96 (34). Recent studies on Antia have shown its ability to reverse oxidative-stress-induced
97 mitochondrial dysfunction in human peripheral blood lymphocytes (35). In light of the above-
98 mentioned neuroprotective effects of Antia's plant components, we hypothesized that Antia would
99 have beneficial effects on the pathways relevant to AD, namely the oxidative stress, amyloidogenic,
100 inflammatory, and autophagy pathways. We studied the effect of Antia on mice induced with
101 SAD via intracerebroventricular (ICV) injection of streptozotocin (STZ); this is a well-established
102 animal model of SAD based on brain resistance to insulin (36) and imitates the age-related
103 pathology of SAD in humans such as memory impairment, oxidative stress, neuroinflammation,
104 and neurodegeneration (37). Here we present behavioral, biochemical, and Western blot
105 experiments in support of our hypothesis.

106

107

Methods

108

Animals

110 Adult male albino mice weighing 25-30 g were provided by the animal facility of the Faculty of
111 Pharmacy, Cairo University, Egypt, and they were allowed to acclimate for one week before
112 conducting the study. Animals were housed in controlled environmental conditions of constant
113 temperature (25 ± 2 °C), relative humidity of $60 \pm 10\%$, and light/dark cycle (12/12-h). Standard
114 chow diet and water were allowed ad libitum. All efforts were utilized to minimize animal
115 suffering and to reduce the number of animals used. This study was approved by the Ethics
116 Committee for Animal Experimentation (Faculty of Pharmacy, Cairo University) and complied
117 with the recommendations of the National Institutes of Health Guide for Care and Use of
118 Laboratory Animals (2011).

119

120 Chemicals

121 STZ was purchased from Sigma–Aldrich Co. (St Louis, MO, USA). STZ was dissolved in saline
122 solution (0.9% NaCl) and injected ICV at a volume of 10 μ L by the freehand method. Antia was
123 dissolved in saline solution in three doses: 25mg/kg equivalent to the adult dose (4 tablets/day),
124 50 mg/kg, and 100 mg/kg. It was then administered intraperitoneally (i.p.) at a volume of
125 0.1ml/20g-mouse. Fresh drug solutions were prepared on each day of experimentation. The control
126 group received saline injections of the same volume and through the same routes of administration.
127 All other chemicals were of the highest analytical grade.

128

129 Antia

130 Antia is a natural compound derived from a variety of mushrooms and plants, including the edible
131 yamabushitake mushroom, the gotsukora and kothala himbutu plants, diosgenin (an extract from
132 the tubers of dioscorea wild yam), and amla (Indian gooseberry). The ingredients are treated with
133 an iron-based fluid called MRN-100. MRN-100 is made from phytosin and is an iron-based
134 compound derived from bivalent and trivalent ferrates (hydroferrate fluid). The exact chemical
135 composition of Antia is still under active investigation. Antia was provided by ACM Co., Ltd,
136 Japan. Antia was prepared in distilled water (DW) with the concentration of MRN-100 at about 2
137 $\times 10^{-12}$ mol/L.

138

139 Induction of SAD

140 SAD was induced by ICV injection of STZ (3 mg/kg) into the lateral ventricle of mice according
141 to the freehand procedure (38) and as updated by Warnock et al. (39) to avoid the probability of

142 cerebral vein penetration. After mice were anesthetized with thiopental (5 mg/kg, i.p.), the head
143 was stabilized using downward pressure above the ears and the needle was inserted directly
144 through the skin and skull into the lateral ventricle which was targeted by visualizing an equilateral
145 triangle between the eyes and the center of the skull to locate the bregma, allowing the needle to
146 be inserted about 1mm lateral to this point. Mice behaved normally one minute following the
147 injection.

148

149 **Experimental design**

150 The experimental design is illustrated in Figure 1. Mice were randomly divided into five groups,
151 each containing 12 animals. Group I (Control): mice received ICV injection once and
152 intraperitoneal (i.p.) saline injection for 21 consecutive days and served as normal control group.
153 Group II (STZ): mice received STZ (3 mg/kg, ICV) once and served as a model for SAD (40).
154 Group III (STZ+Antia 1): mice received STZ (3 mg/kg, ICV) followed by Antia (25 mg/kg, i.p)
155 after five hours and then every day for 21 consecutive days. Group IV (STZ+Antia 2): mice
156 received STZ (3 mg/kg, ICV) followed by Antia (50 mg/kg, i.p) after five hours and then every
157 day for 21 consecutive days. Group V (STZ+Antia 3): mice received STZ (3 mg/kg, ICV) followed
158 by Antia (100 mg/kg, i.p) after five hours and then every day for 21 consecutive days. Twenty-
159 four hours after the end of the treatments, neurobehavioral tests were carried out, including object
160 recognition and Morris water maze (MWM) tests, arranged in sequence from the least stressful
161 test to the most stressful test. To minimize possible circadian variability, all testing was conducted
162 during the animals' light cycle under top illumination.

163

164 **Behavioral assessments**

165 **Object recognition test.** The object recognition test is used to assess long-term memory and
166 estimate cognition (41). In this study, the performed test took place on three consecutive days. On
167 the first day (the habituation phase), each mouse was individually placed in a wooden box of
168 dimensions 30x30x30 cm³ for 30 min in order to adapt to the surrounding environment. The second
169 day was designated for the familiarization or training, where two wooden cubes identical in shape,
170 color, and size were placed in opposite corners of the box, 2 cm from the walls. Each mouse was
171 placed in the middle of the box and was left to explore these two objects for 10 min. On the third
172 day, testing took place. One of the two identical cubes was replaced by a novel object that was
173 different in shape, size, and color. Each mouse was exposed again to these two objects for 5 min.
174 Objects added were cleaned with 70% ethanol between experiments with animals to ensure that
175 the behavior was not guided by odor cues. All objects and locations were adjusted to decrease
176 potential biases due to inclinations for particular locations or objects. A mouse could not displace
177 the objects and the subjects were always placed into the box confronting the same wall. The
178 animals' behavior was video-recorded and the following parameters were calculated:

- 179 1) Discrimination index: Difference in time exploring the novel and familiar objects divided by
180 the total time spent exploring both objects. This result varies between +1 and -1, where a
181 positive score indicates more time spent with the novel object, a negative score shows more
182 time spent with the familiar object, and a zero score indicates a null preference.
- 183 2) Recognition index: Time spent by the animal exploring the novel object as a percentage of the
184 total exploration time for both objects.

185

186 **Morris water maze test.** The MWM test is used to investigate spatial learning and memory in
187 laboratory mice (42). The maze consisted of stainless-steel circular tanks (210 cm in diameter, 51

188 cm high) divided into four quadrants and filled with water ($25 \pm 2^{\circ}\text{C}$) to a depth of 35 cm. A
189 submerged platform (10 cm width, 28 cm height), painted in black, was placed inside the target
190 quadrant, 2 cm below the water surface. The platform was kept at a consistent position during the
191 time of training and the test. A purple-colored non-toxic dye was added to make the water opaque
192 so that the platform was made invisible. Memory-acquisition trials (120 s/trial) were performed
193 two times a day for four consecutive days, with an interval of at least 15 min between the trials.
194 During each acquisition trial, animals were left free to locate the hidden platform in the target
195 quadrant. Once the mouse located the platform, it was left there for an additional 20 s to rest, while
196 if an animal failed to reach the platform within 120 s, it was gently guided to the platform and kept
197 there for 20 s. The mean escape latency was calculated as the time taken by each rat to find the
198 hidden platform and was used as an index of acquisition or learning. On the fifth day, the mice
199 were subjected to a probe-trial session where the platform was taken away from the pool and each
200 rat was allowed to probe the pool for 60 s. The time spent by each rat in the target quadrant in
201 which the hidden platform was previously placed was recorded as an indicator of retrieval or
202 memory.

203

204 **Brain processing**

205 After behavioral testing, mice were euthanized by cervical dislocation and brains were rapidly
206 dissected and washed with ice-cold saline. The hippocampi (n=6) were excised from each brain
207 on an ice-cold glass plate. The hippocampus was homogenized in ice-cold saline to prepare 10%
208 homogenates that were divided into several aliquots and stored at -80°C . The other hippocampus
209 was stored at -80°C to be used for Western blot analysis.

210

211 **Biochemical measurements**

212 ***Determination of oxidative stress and inflammatory biomarkers.*** Hippocampal lipid peroxidation
213 was estimated by measuring the level of malondialdehyde (MDA). MDA was determined by
214 measuring the thiobarbituric acid reactive substances according to the method described by
215 Uchiyama and Mihara (43). Moreover, the brain glutathione (GSH) content was
216 spectrophotometrically determined using Ellman's reagent according to the method described by
217 Beutler et al. (44). The results are expressed as Mmol/mg protein.

218
219 ***Enzyme-linked immunosorbent assay.*** Hippocampal TNF- α and IL-6 levels were estimated using
220 rat ELISA kits purchased from RayBiotech Inc. (Norcross, GA, USA) and R&D Systems Inc.
221 (Minneapolis, USA), respectively. The procedures were performed according to the manufacturers'
222 instructions. The results are presented as pg/mg protein for both TNF- α and IL-6.

223
224 ***Western blot analysis.*** After protein solutions were extracted from the brain tissues, equal amounts
225 of protein (20–30 μ g of total protein) were separated by SDS-PAGE (10% acrylamide gel) and
226 transferred to polyvinylidene difluoride membranes (Pierce, Rockford, IL, USA) with a Bio-Rad
227 Trans-Blot system. Immunodetection of Western blots was conducted by incubating the
228 membranes at room temperature for 1 h with blocking solution comprised of 20 mM Tris-Cl, pH
229 7.5, 150 mM NaCl, 0.1% Tween 20 and 3% bovine serum albumin. Membranes were incubated
230 overnight at 4°C with one of the following primary antibodies: P-JAK2 (Tyr 1007/1008), P-
231 STAT3 (Tyr 705), I κ B- α , GSK-3 β , mTOR, COX-2, or β -actin, obtained from Thermo Fisher
232 Scientific Inc. (Rockford, IL, USA). After washing, peroxidase-labelled secondary antibodies
233 were added and the membranes were incubated at room temperature for 1 h. The band intensity

234 was analyzed using ChemiDoc™ imaging system with Image Lab™ software version 5.1 (Bio-
235 Rad Laboratories Inc., Hercules, CA, USA). The results are presented in arbitrary units after
236 normalization to levels of the β -actin protein.

237

238 ***Determination of protein content.*** Protein content was measured according to the method of
239 Bradford. All the results are expressed as tissue concentration per mg protein.

240

241 **Statistical analysis**

242 The data are presented as mean \pm S.E. Data were analyzed using one-way analysis of variance
243 (ANOVA) followed by the Tukey-Kramer multiple comparison test. GraphPad Prism software
244 (version 6; GraphPad Software, Inc., San Diego, CA, USA) was used to perform the statistical
245 analysis and create the graphical presentations. The level of significance was set to $p < 0.05$ for all
246 statistical tests.

247

248

Results

249

250 The effects of Antia on the behavioral and biochemical functions of ICV-STZ treated mice
251 were measured with neurobehavioral tests and biochemical analysis of the hippocampal content.
252 The effects of STZ and Antia (25, 50 and 100 mg/kg) on neurobehavioral tests were carried out
253 within 24h after the last day of Antia injection. The Morris water maze was used to examine the
254 possible protective effect of Antia treatment on ICV-STZ injected mice. As illustrated in Figure
255 2A for the mean escape latency (MEL), mice in different groups took different times to escape on
256 day 2. Alzheimer's mice took 1.63 times as long to escape on day 2 as compared to control mice.

257 On the other hand, Alzheimer's mice with Antia took only 1.08 times as long as control mice on
258 day 2. These results were further confirmed in the subsequent days 3 and 4. The study of the effect
259 of Antia on the time mice spent in the target quadrant of the Morris water maze (Figure 2B) showed
260 that Alzheimer's mice spent only 25.4% of the time in the quadrant as compared to control mice,
261 while Alzheimer's mice with 25, 50, and 100 mg/kg of Antia spent 72.5%, 75.8%, and 85.4% of
262 the time, respectively, as compared to control mice.

263 The effect of STZ and Antia was further examined through the discrimination and
264 preference indices of the novel object recognition test. The discrimination index was decreased in
265 STZ-induced SAD mice when compared to the control group, but it was significantly increased
266 after Antia administration (25, 50, and 100mg/kg) as compared to the STZ group in a dose
267 dependent manner. In addition, the time spent exploring the novel object was lower in ICV-STZ
268 injected mice by 63% compared to the control group, reflecting a lower preference index. Antia
269 administration (25, 50 and 100mg/kg) normalized the preference index, indicating that Antia-
270 treated mice preferred the novel object over the familiar object in a dose dependent manner (Figure
271 2C).

272 Several biochemical analyses of the hippocampal content in ICV-STZ treated mice were
273 conducted in order to examine the ability of Antia to attenuate the amyloidogenic, inflammatory,
274 autophagy and oxidative stress pathways. Studies on the protective effect of Antia treatments on
275 the levels of glutathione (GSH) and malondialdehyde (MDA) hippocampal content were carried
276 out. Results in Figure 3A show that Alzheimer's mice had a GSH level that was 15.5% of the
277 GSH level of control mice. On the other hand, Alzheimer's mice with Antia showed an elevation
278 in the GSH content in a dose dependent manner that maximized at 78.7% of the control GSH level
279 for 100 mg/kg Antia treatment. Results of the levels of MDA hippocampal content show

280 significantly higher levels of MDA in ICV-STZ injected mice as compared with control mice by
281 a factor of 4.3 fold. On the other hand, Alzheimer's mice with Antia showed an elevation in the
282 MDA content of only 3.5 fold, 2.5 fold, and 1.8 fold for mice receiving Antia at doses of 25, 50
283 and 100 mg/kg respectively (Figure 3B).

284 The effect of ICV-STZ injection on the hippocampal content of anti-inflammatory
285 cytokines was also examined in the presence and absence of Antia treatment. Two cytokines were
286 examined: TNF- α and IL-6. Results in Figure 4 show that STZ model mice exhibited a significant
287 increase in the expression of TNF- α and IL-6 cytokines as compared with control mice, but
288 treatment with Antia suppressed this induction in a dose dependent fashion that reached the level
289 of control at 100 mg/kg. A similar trend can also be seen in the hippocampal content of NF- κ B
290 p65. Results in Figure 4 show increased levels of NF- κ B p65 in the Alzheimer's mice and its
291 gradual decrease in Alzheimer's mice with Antia.

292 Since amyloid β makes up the plaques of Alzheimer's disease, where these normally solid
293 proteins assemble into amyloid-like filaments, we examined the effect of Antia on Amyloid β_{1-42}
294 hippocampal content in ICV-STZ injected mice. Results depicted in Figure 5 show that STZ model
295 mice exhibited an approximately 4 fold increase in the expression of amyloid β as compared with
296 control mice. It is of interest to note that the levels of amyloid β were significantly decreased in
297 Alzheimer's mice with Antia. The effect was dose dependent and reached its lowest levels at 100
298 mg/kg.

299 We further examined protein expression. The levels of phosphorylation of STAT and JAK
300 protein expression is a well-established method used in Alzheimer's research. We examined
301 whether treatment with Antia suppresses the phosphorylation of STAT expression in STZ mice.
302 As expected, the levels of phosphorylation of STAT protein expression was significantly reduced

303 as compared with control mice. However, treatment of STZ mice with Antia resulted in a
304 significant inhibition in the phosphorylation level of STAT3 (Figure 6A). A similar trend in results
305 was observed with JAK2 protein expression. Treatment with Antia caused a significant inhibition
306 in the phosphorylation level of JAK2 due to of STZ injection (Figure 6A). These results indicate
307 the protective effect of Antia for the JAK2/STAT3 pathway.

308 Earlier studies have shown that glycogen synthase kinase-3 (GSK-3) phosphorylates tau
309 protein, the principal component of neurofibrillary tangles. Inhibition of GSK-3a offers a new
310 approach to reduce the formation of both amyloid plaques and neurofibrillary tangles, two
311 pathological hallmarks of Alzheimer's disease (45). Results in Figure 6B show that Alzheimer's
312 mice had a higher expression of GSK-3 β level that was 7 fold larger than the GSK-3 β level of
313 control mice. On the other hand, treatment with Antia caused a dramatic inhibition in the
314 expression of GSK-3 β that was approximately 3 fold of the control. Results in Figure 6B also
315 show that Alzheimer's mice had a higher expression of IKB- α that approximately 6.5 fold larger
316 than the IKB- α level of the control mice. On the other hand, treatment with Antia caused a dramatic
317 inhibition in the expression of IKB- α that was approximately 2.8 fold of the control.

318 Several studies have shown that the mammalian target of rapamycin (mTOR) may play a
319 role in amyloid β and tau induced neurodegeneration (46). Earlier studies showed higher levels of
320 mTOR phosphorylated at Ser2481 in the medial temporal cortex of AD cases compared to control
321 cases (47-48). Results in Figure 6C showed that STZ injected mice exhibited significantly
322 increased levels of the mTOR and p-AKT protein expression that were 5x and 6x greater than the
323 level of control mice, respectively, but treatment with Antia reversed that increase and brought it
324 close to that of the control values.

325 Finally, COX-2 is a key enzyme in the inflammatory processes. Results in Figure 6D show
326 that Alzheimer's mice exhibited a significant induction in COX-2 expression, 600% of the COX-
327 2 level of control mice. Treatment with Antia, however, significantly reduced the expression of
328 COX-2 to 150%-300%.

329

330

331

Discussion

332

333 Results of the present study demonstrate the ability of the anti-oxidant Antia to exert a
334 protective effect against SAD induced in mice. The constituents of Antia have previously been
335 shown to possess various neuro-regenerative and protective properties. Yamabushitake
336 mushrooms have been shown to synthesize nerve growth factor (49-51); gotsukora extracts reduce
337 the amyloid β levels in the Alzheimer's-stricken brains of laboratory animals (23); diosgenin
338 enhances the cognitive performance of mice (27); amla acts as a potent anti-oxidant with strong
339 neuro-protective effects and cognitive enhancement properties (28-30); and kothala himbutu
340 protects against deleterious cognitive changes in young diabetic rats (31) and against mercury
341 toxicity in mice hippocampi (32). Here, Antia is shown to attenuate cognitive dysfunction in the
342 mouse model by targeting several linked pathways, including the amyloidogenic, inflammatory,
343 autophagy, and oxidative stress pathways.

344 In the present study, induction of SAD in mice by STZ induced a significant cognitive
345 decline in the Morris water maze and novel object recognition tests. ICV injection of STZ is an
346 experimental model that mimics the progressive pathology of SAD similar to human brains (37).
347 STZ-treated mice showed significant learning and memory deficits, as shown by the noticeable

348 inability of mice to discriminate between familiar and novel objects in the Morris water maze and
349 novel object recognition tasks. This is in harmony with previous studies (52-53). However, the
350 profound elevation in escape latency during the acquisition trial and the time spent in the target
351 quadrant during the probe trail in the Morris water maze test, as well as the increase in
352 discrimination and preference indices in the novel object recognition test, proved that Antia
353 prevented the STZ-induced impairments of spatial and short term memory. This improvement in
354 the object recognition memory deficit could be attributed to the previously proven effects of
355 several of Antia's ingredients. For example, it has been shown that diosgenin has an anti-
356 amyloidogenic effect (27,54) and that *Herichium erinaceus* has a strong neuroprotective effect
357 against neuronal loss and dementia in AD (55-56). Furthermore, oral administration of dried
358 yamabushitake mushroom powder has been demonstrated to be effective in improving mild
359 cognitive impairment in humans (19).

360 STZ administration exhibited a significant increase in the expression of the hippocampal
361 content of NF- κ B and anti-inflammatory cytokines, namely TNF- α and IL-6. NF- κ B plays a
362 crucial role in the inflammatory responses in neurons where it induces the transcription of
363 inflammatory target genes, including COX-2, IL-1 β , IL-6, and TNF- α (57). TNF- α is involved in
364 systemic inflammation, and in particular, it is involved in AD-related brain neuroinflammation as
365 well as amyloidogenesis via β -secretase regulation. Moreover, profound neuropathological
366 changes such as Parkinson's and Alzheimer's disease are associated with increased IL-6 expression
367 in the brain (58). NF- κ B has also been shown to regulate the BACE-1 expression level, the rate-
368 limiting enzyme responsible for the production of amyloid β . The Janus Kinase/Signal Transducers
369 and Activators of Transcription (JAK/STAT) signaling pathway emerged in the 1980s as the
370 pathway mediating interferon signaling. Neuroinflammation is accompanied by diseases, and

371 activation of the JAK2/STAT3 pathway leads to pathogenic inflammation. Thus, targeting the
372 JAK2/STAT3 pathway can be used as a protective therapy for neuroinflammatory and
373 neurodegenerative diseases such as AD.

374 In the present study, administration of Antia was shown to have a significant anti-
375 inflammatory effect, as demonstrated by decreasing the levels of all measured inflammatory
376 cytokines as well as dramatically inhibiting the expression of phosphorylated STAT3 and JAK2.
377 The STAT3/JAK2 pathway has been linked to TNF- α production (59-60). The significant
378 inhibition of TNF- α and NF- κ B might be attributed to the action of *Herichium erinaceus*, known as
379 yamabushitake, which has been shown to play an important role in transcriptional regulation of
380 adhesion molecules and numerous cytokines including IL-6 and TNF- α (61-62).

381 Neuroinflammation has been linked to a deficit of autophagy, which may contribute to
382 neurodegeneration (8). The mammalian target of rapamycin (mTOR) is known to regulate
383 autophagy, along with protein kinase B (Akt) (63). Several studies emphasize the close relationship
384 between mTOR signaling and the presence of amyloid β plaques and cognitive impairment in AD
385 (64-67). Furthermore, in human and rat studies of AD, autophagy activation has been linked to
386 GSK-3 β inhibitors and its deficit has been found to contribute to the pathological accumulation of
387 tau aggregates (9,11).

388 Treatment with Antia reversed the elevated expression of mTOR, Akt, I κ B- α , and GSK-3 β
389 levels after STZ injection and brought it to closer that of the control. Recent reports showed that
390 increasing the axonal density of neurons by diosgenin caused a significant improvement in
391 cognitive function. This could be achieved through modulation of the PI3K-Akt pathway, which
392 is known to regulate local protein translation via the mTOR pathway, thus playing an important
393 role in axon regeneration (27,68).

394 Results of this study showed that Antia increases GSH and decreases lipid peroxidation in
395 STZ-treated mice. Previous research showed that the generation of ROS via amyloid β during
396 self-aggregation may damage neurons and cause neuronal death (69). Lipid peroxidation is
397 considered to be one of the major outcomes of free radical-mediated injury that directly damages
398 membranes, and increased lipid peroxidation has been reported in the brain of AD patients (70-
399 71). Treatment of STZ-treated mice with Antia improved the oxidative stress parameters. This
400 might be attributed to its previously known ability to reverse oxidative-stress-induced
401 mitochondrial dysfunction and apoptosis (35). In addition, centella asiatica, commonly known as
402 gotsukora, has been found previously to exhibit noticeable free radical scavenging properties,
403 decreased lipid peroxidation, and protection from DNA fragmentation due to oxidative stress,
404 providing multiple mechanisms to alter pathology in Alzheimer's brain (23). Previous studies have
405 shown the beneficial anti-oxidant properties of MRN-100, the hydroferrate fluid that is used to
406 treat Antia's constituents, to increase brain levels of GSH, superoxide dismutase, catalase, and
407 glutathione peroxidase and to inhibit of the levels of oxidative stress biomarkers including MDA,
408 nitric oxide, and total free radicals (33). GSH is an anti-oxidant that has the ability to prevent
409 damage caused by ROS and may protect against oxidative and neurotoxic degeneration of
410 oligomeric amyloid β (72-73).

411 It could be concluded from the present study that Antia exerts a significant protection against
412 sporadic AD induced by ICV injection of STZ. This effect is achieved through targeting the
413 amyloidogenic, inflammatory, and oxidative stress pathways. The JAK2/STAT3 pathway played
414 a protective role for the induced neuroinflammation, which is mediated through modulation of the
415 Akt/mTOR/GSK-3 β pathway. To our knowledge, this is the first work done to investigate the
416 protective effect of Antia against neurodegenerative diseases such as SAD.

Acknowledgements

The authors acknowledge ACM Co., Ltd., Japan, for providing Antia and Dr. B. J. Winjum at UCLA for help in preparing the manuscript.

Authors' Contributions

N. S. and M. G. designed research, N. S. conducted research, and N. S. and M. G. analyzed data and wrote the paper. N. S. and M. G. had equal responsibility for final content. Both read and approved the final manuscript.

References

1. Patterson C: World Alzheimer Report 2018: The state of the art of dementia research: new frontiers. Alzheimer's Disease International, London, 2018.
2. Blennow K, de Leon MJ, Zetterberg H. Alzheimer's disease. *Lancet*. 2006;368(9533):387-403.
3. Nunomura A, Perry G, Pappolla MA, Friedland RP, Hirai K, Chiba S, Smith MA. Neuronal oxidative stress precedes amyloid-beta deposition in Down syndrome. *J Neuropathol Exp Neurol*. 2000 Nov;59(11):1011-7.
4. Polidori MC. Oxidative stress and risk factors for Alzheimer's disease: clues to prevention and therapy. *J Alzheimers Dis*. 2004;6:185-91.
5. Bélanger M, Allaman I, and Magistretti PJ. Brain energy metabolism: focus on astrocyte-neuron metabolic cooperation. *Cell Metabolism*. 2011;14:724-38.
6. Mattson MP. Pathways towards and away from Alzheimer's disease. *Nature*. 2004;430(7000):631-9.

7. Flagmeier P, De S, Wirthensohn DC, Lee SF, Vincke C, Muyldermans S, Knowles TP, Gandhi S, Dobson CM, Klenerman D. Ultrasensitive Measurement of CA^{2+} Influx into Lipid Vesicles Induced by Protein Aggregates. *Angewandte Chemie*. 2017;56(27):7750-4.
8. Zheng HF, Yang YP, Hu LF, Wang MX, Wang F, Cao LD, Li D, Mao CJ, Xiong KP, Wang JD, Liu CF. Autophagic impairment contributes to systemic inflammation-induced dopaminergic neuron loss in the midbrain. *PLoS One*. 2013;8(8):e70472.
9. Zare-Shahabadi A, Masliah E, Johnson GV, Rezaei N. Autophagy in Alzheimer's disease. *Reviews in the Neurosciences*. 2015;26:385–95.
10. Srivastava, IN, Shperdheja, J, Baybis, M, Ferguson T, and Crino, PB. mTOR pathway inhibition prevents neuroinflammation and neuronal death in a mouse model of cerebral palsy. *Neurobiology of Disease*. 2016;85:144–54.
11. Zhou, X., Zhou, J., Li, X., Guo, C.'a., Fang, T., and Chen, Z. GSK-3 β inhibitors suppressed neuroinflammation in rat cortex by activating autophagy in ischemic brain injury. *Biochem Biophys Res Commun*. 2011 Jul 29;411(2):271-5.
12. Szekely CA, Town T, Zandi PP. NSAIDs for the chemoprevention of Alzheimer's disease. *Sub-Cellular Biochemistry*. *Subcell Biochem*. 2007;42:229-48.
13. Hsu D, Marshall GA. Primary and Secondary Prevention Trials in Alzheimer Disease: Looking Back, Moving Forward. *Curr Alzheimer Res*. 2017;14(4):426-440.
14. Markesbery WR. The Role of Oxidative Stress in Alzheimer Disease. *Arch Neurol*. 1999 Dec;56(12):1449-52.
15. Gugliandolo A, Bramanti P and Mazzon E. Role of Vitamin E in the Treatment of Alzheimer's Disease: Evidence from Animal Models. *Int J Mol Sci*. 2017 Nov 23;18(12). pii: E2504.

16. Choi SY, Lim SH, Kim JS, Ha TY, Kim SR, Kang KS, Hwang IK. Evaluation of the estrogenic and antioxidant activity of some edible and medicinal plants. *Korean J Food Sci Technol.* 2005;37:549–56.
17. Kawagishi H, Ando M, Mizuno T. Hericenone A and B as cytotoxic principles from the mushroom *hericium erinaceum*. *Tetrahedron Lett.* 1990;31:373–6.
18. Kawagishi H, Shimada A, Shirai R, Okamoto K, Ojima F, Sakamoto H, Ishiguro Y, Furukawa S. Erinacines A, B and C, strong stimulators of nerve growth factor (NGF)-synthesis, from the mycelia of *Herichium erinaceum*. *Tetrahedron Lett.* 1994;35:1569–72.
19. Mori K, Inatomi S, Ouchi K, Azumi Y, Tuchida T. Improving effects of the mushroom Yamabushitake (*Herichium erinaceus*) on mild cognitive impairment: a double-blind placebo-controlled clinical trial. *Phytother. Res.* 2009;23:367–72.
20. Nadkarni, K. M., and A. K. Nadkarni. Dr. K.M. Indian Materia Medica. Bombay Popular Prakashan, 1954.
21. K R Kirtikar, B D Basu, and E Blatter. Indian Medicinal Plants. Dehradun : International Books Distributors, 1987.
22. Gupta YK, Kumar MHV, Srivastava AK. Effect of *Centella asiatica* on pentylentetrazole-induced kindling, cognition and oxidative stress in rats. *Pharmacol Biochem Behav.* 2003;74:579-85.
23. Dhanasekaran M, Holcomb LA, Hitt AR, Tharakan B, Porter JW, Young KA, Manyam BV. *Centella asiatica* extract selectively decreases amyloid beta levels in hippocampus of Alzheimer's disease animal model. *Phytother Res.* 2009;23:14-9.
24. McGeer PL, McGeer EG. The amyloid cascade-inflammatory hypothesis of Alzheimer disease: implications for therapy. *Acta Neuropathol.* 2013;126:479–97.

25. Zhu X, Su B, Wang X, Smith MA, Perry G. Causes of oxidative stress in Alzheimer disease. *Cell Mol Life Sci.* 2007;64:2202–10.
26. Bush AI. Drug development based on the metals hypothesis of Alzheimer's disease. *J Alzheimers Dis.* 2008;15:223–40.
27. Tohda C, Lee YA, Goto Y, Nemere I. Diosgenin-induced cognitive enhancement in normal mice is mediated by 1,25D₃-MARRS. *Sci Rep.* 2013 Dec 2;3:3395.
28. Ali SK, Hamed AR, Soltan MM, Hegazy UM, Elgorashi EE, El-Garf IA, Hussein AA. In-vitro evaluation of selected Egyptian traditional herbal medicines for treatment of Alzheimer disease. *BMC Complement Altern Med.* 2013;13:121.
29. Liu W, Ma H, DaSilva NA, Rose KN, Johnson SL, Zhang L, Wan C, Dain JA, Seeram NP. Development of a neuroprotective potential algorithm for medicinal plants. *Neurochem Int.* 2016;100:164-77.
30. Uddin MS, Mamun AA, Hossain MS, Akter F, Iqbal MA, Asaduzzaman M. Exploring the Effect of *Phyllanthus emblica* L. on Cognitive Performance, Brain Antioxidant Markers and Acetylcholinesterase Activity in Rats: Promising Natural Gift for the Mitigation of Alzheimer's Disease. *Ann Neurosci.* 2016;23(4):218-29.
31. Rajashree R, Patil R, Khlokute SD, Goudar SS. Effect of *Salacia reticulata* W. and *Clitoria ternatea* L. on the cognitive and behavioral changes in the streptozotocin-induced young diabetic rats. *J Basic Clin Physiol Pharmacol.* 2017;28(2):107-14.
32. Tams GE, Kani JN, Blessing CD, Peter AS. Antidegenerative and Neurobehavioral Effects of Ethanolic Root Extract of *Salacia reticulata* on Mercury Chloride Induced Cellular Damage in the Hippocampus of Adult Male Mice. *J Cytol Histol.* 2018;9:3.

33. Badr El-Din NK, Noaman E, Fattah SM, Ghoneum M. Reversal of age-associated oxidative stress in rats by MRN-100, a hydro-ferrate fluid. *In Vivo*. 2010;24:525-33.
34. Lin F, Girotti AW. Elevated ferritin production, iron containment, and oxidant resistance in hemin-treated leukemia cells. *Arch Biochem Biophys*. 1997 Oct 1;346(1):131-41.
35. Ghoneum MH. Reversal of oxidative-stress-induced mitochondrial dysfunction and apoptosis in human peripheral blood lymphocytes by Antia, a naturally-derived anti-oxidant. AAIC Conference Los Angeles CA (2019).
36. Salkovic-Petrisic M, Knezovic A, Hoyer S, Riederer P. What have we learned from the streptozotocin-induced animal model of sporadic Alzheimer's disease, about the therapeutic strategies in Alzheimer's research. *J Neural Transm (Vienna)*. 2013;120(1):233-52.
37. Kamat PK, Kalani A, Rai S, Tota SK, Kumar A, Ahmad AS. Streptozotocin Intracerebroventricular-Induced Neurotoxicity and Brain Insulin Resistance: a Therapeutic Intervention for Treatment of Sporadic Alzheimer's Disease (sAD)-Like Pathology. *Mol Neurobiol*. 2016;53:4548-62.
38. Pellemounter MA, Joppa M, Ling N, Foster AC. Pharmacological evidence supporting a role for central corticotropin-releasing factor(2) receptors in behavioral, but not endocrine, response to environmental stress. *J Pharmacol Exp Ther*. 2002;302:145-52.
39. Warnock GI. Study Of The Central Corticotrophin-Releasing Factor System Using The 2-Deoxyglucose Method For Measurement Of Local Cerebral Glucose Utilisation. Dissertation. University of Bath (2010).
40. Mehla J, Pahuja M, Gupta YK. Streptozotocin-Induced Sporadic Alzheimer's Disease: Selection of Appropriate Dose. *J Alzheimer's Dis*. 2012;33:17-21.

41. Ennaceur A. One-trial object recognition in rats and mice : Methodological and theoretical issues. *Behav Brain Res.* 2010;215:244–54.
42. Morris GM. Spatial Localization Does Not Require Local Cues the Presence of Local Cues. *Learn Motiv.* 1981;260:239–60.
43. Mihara M, Uchiyama M. Determination of malonaldehyde precursor in tissues by thiobarbituric acid test. *Anal Biochem.* 1978 May;86(1):271-8.
44. Beutler E, Duron O, Kelly BM. Improved method for the determination of blood glutathione. *J Lab Clin Med.* 1963 May;61:882-8.
45. Phiel CJ, Wilson CA, Lee VM, Klein PS. GSK-3a regulates production of Alzheimer's disease amyloid- β peptides. *Nature.* 2003;423(6938):435-9.
46. Oddo S. The role of mTOR signaling in Alzheimer disease. *Front Biosci (Schol Ed).* 2012;4:941-52.
47. Li X, Alafuzoff I, Soininen H, Winblad B, Pei JJ. Levels of mTOR and its downstream targets 4E-BP1, eEF2, and eEF2 kinase in relationships with tau in Alzheimer's disease brain. *FEBS J.* 2005 Aug;272(16):4211-20.
48. Griffin RJ, Moloney A, Kelliher M, Johnston JA, Ravid R, Dockery P, O'Connor R, O'Neill C. Activation of Akt/PKB, increased phosphorylation of Akt substrates and loss and altered distribution of Akt and PTEN are features of Alzheimer's disease pathology. *J Neurochem.* 2005;93:105–17.
49. Mori K, Obara Y, Hirota M, Azumi Y, Kinugasa S, Inatomi S, Nakahata N. Nerve growth factor-inducing activity of *Hericium erinaceus* in 1321N1 human astrocytoma cells. *Biol Pharm Bull.* 2008;31:1727-32.

50. Ma B-J, Shen J-W, Yu H-Y, Ruan Y, Wu T-T, and Zhao X. Hericenones and erinacines: stimulators of nerve growth factor (NGF) biosynthesis in *Herichium erinaceus*. *Mycology*. 2010;1:92-8.
51. Spelman K, Sutherland E, Bagade A. Neurological Activity of Lion's Mane (*Herichium erinaceus*). *J Restorative Med*. 2017;6:19-26.
52. Halawany AME, Sayed NSE, Abdallah HM, Dine RSE. Protective effects of gingerol on streptozotocin-induced sporadic Alzheimer's disease: emphasis on inhibition of β -amyloid, COX-2, alpha-, beta - secretases and A β 1a. *Sci Rep*. 2017;7(1):2902.
53. Abdel Rasheed NO, El Sayed NS, El-Khatib AS. Targeting central β 2 receptors ameliorates streptozotocin-induced neuroinflammation via inhibition of glycogen synthase kinase3 pathway in mice. *Prog Neuro-Psychopharmacology Biol Psychiatry*. 2018;86:65–75.
54. Lecanu L, Rammouz G, McCourty A, Sidahmed EK, Greeson J, Papadopoulos V. Caprospinol reduces amyloid deposits and improves cognitive function in a rat model of Alzheimer's disease. *Neuroscience*. 2010 Jan 20;165(2):427-35.
55. Nagai K, Chiba A, Nishino T, Kubota T, Kawagishi H. Dilinoleoyl -phosphatidylethanolamine from *Herichium erinaceus* protects against ER stress-dependent Neuro2a cell death via protein kinase C pathway. *J Nutr Biochem*. 2006;17:525–30.
56. Kawagishi H, Zhuang C. Compounds for dementia from *Herichium erinaceum*. *Drugs Future*. 2008;33:149–55.
57. Xiao C., Ghosh S. NF-kappaB, an evolutionarily conserved mediator of immune and inflammatory responses. *Adv Exp Med Biol*. 2005;560:41–5.

58. Q Alam, MZ Alam, G Mushtaq, GA Damanhour, M Rasool, MA Kamal, and A Haque. Inflammatory Process in Alzheimer's and Parkinson's Diseases: Central Role of Cytokines. *Curr Pharm Des.* 2016;22(5):541-8.
59. Huang C, Ma R, Sun S. JAK2-STAT3 signaling pathway mediates thrombin-induced proinflammatory actions of microglia in vitro. *J Neuroimmunol.* 2008;204(1–2):118–25.
60. Nishiki S, Hato F, Kamata N, Selective activation of STAT3 in human monocytes stimulated by G-CSF: implication in inhibition of LPS-induced TNF- α production. *Am J Physiol Cell Physiol.* 2004;286:C1302–11.
61. Thongbai B, Rapior S, Hyde KD, Wittstein K, Stadler M. *Herichium erinaceus*, an amazing medicinal mushroom. *Mycological Progress.* 2015;14:91.
62. Diling C, Tianqiao Y, Jian Y, Chaoqun Z, Ou S, Yizhen X. Docking Studies and Biological Evaluation of a Potential β -Secretase Inhibitor of 3-Hydroxyhericenone F from *Herichium erinaceus*. *Front Pharmacol.* 2017;8:219.
63. Jung CH, Ro SH, Cao J, Otto NM, Kim DH. mTOR regulation of autophagy. *FEBS Lett.* 2010;584(7):1287-95.
64. Paccalin, M.; Pain-Barc, S.; Pluchon, C.; Paul, C.; Besson, M.N.; Carret-Rebillat, A.S.; Rioux-Bilan, A.; Gil, R.; Hugon, J. Activated mTOR and PKR kinases in lymphocytes correlate with memory and cognitive decline in Alzheimer's disease. *Dement Geriatr Cogn Disord.* 2006;22:320–6.
65. Cai Z, Zhao B, Li K, Zhang L, Li C, Quazi SH, Tan Y. Mammalian target of rapamycin: A valid therapeutic target through the autophagy pathway for Alzheimer's disease? *J Neurosci Res.* 2012;90:1105–18.

66. Pozueta J, Lefort R, Shelanski ML. Synaptic changes in Alzheimer's disease and its models. *Neuroscience*. 2013;251:51–65.
67. Lafay-Chebassier C, Paccalin M, Page G, Barc-Pain S, Perault-Pochat MC, Gil R, Pradier L, Hugon J. mTOR/p70S6k signalling alteration by Abeta exposure as well as in APP-PS1 transgenic models and in patients with Alzheimer's disease. *J Neurochem*. 2005;94:215–25.
68. Verma P, Chierzi S, Codd AM, Campbell DS, Meyer RL, Holt CE, Fawcett JW. Axonal protein synthesis and degradation are necessary for efficient growth cone regeneration. *J Neurosci*. 2005;25:331–42.
69. Ahmad W, Ijaz B, Shabbiri K, Ahmed F, Rehman S. Oxidative toxicity in diabetes and Alzheimer's disease: mechanisms behind ROS/ RNS generation. *J Biomed Sci*. 2017;24(1):76.
70. Montine TJ, Neely MD, Quinn JF, Beal MF, Markesbery WR, Roberts LJ, Morrow JD. Lipid peroxidation in aging brain and Alzheimer's disease. *Free Radic Biol Med*. 2002;33(5):620-6.
71. Liu Q, Smith MA, Avilá J, DeBernardis J, Kansal M, Takeda A, Zhu X, Nunomura A, Honda K, Moreira PI, et al. Alzheimer-specific epitopes of tau represent lipid peroxidation-induced conformations. *Free Radic Biol Med*. 38(6):746-54 (2005).
72. Monks TJ, Ghersi-Egea J-F, Philbert M, Cooper AJL, Lock EA. Symposium Overview: The Role of Glutathione in Neuroprotection and Neurotoxicity. *Toxicological Sciences* 1999;51:161-77.
73. Lasierra-Cirujeda J, Coronel P, Aza MJ, and Gimeno M. Beta-amyloidolysis and glutathione in Alzheimer's disease. *J Blood Med*. 2013;4:31–8.

Figure Legends

Figure 1: Experimental design.

Figure 2: (A) Effect of Antia on mean escape latency (MEL) in Morris water maze, (B) effect of Antia on time spent in target quadrant in Morris water maze, and (C) effect of Antia on cognitive function in the novel object recognition test for ICV-STZ injected mice.

* Significantly different from normal group at $p < 0.05$

@ Significantly different from ICV-STZ group at $p < 0.05$

Figure 3A&B: Effect of Antia on GSH and MDA hippocampal content in ICV-STZ injected mice.

* Significantly different from normal group at $p < 0.05$

@ Significantly different from ICV-STZ group at $p < 0.05$

Significantly different from Antia (25 mg/kg) at $p < 0.05$

\$ Significantly different from Antia (50 mg/kg) at $p < 0.05$

Figure 4: Effect of Antia on TNF- α , IL-6 and NF- κ B p65 hippocampal content in ICV-STZ injected mice.

* Significantly different from normal group at $p < 0.05$

@ Significantly different from ICV-STZ group at $p < 0.05$

Significantly different from Antia (25 mg/kg) at $p < 0.05$

\$ Significantly different from Antia (50 mg/kg) at $p < 0.05$

Figure 5: Effect of Antia on Amyloid β_{1-42} hippocampal content in ICV-STZ injected mice.

* Significantly different from normal group at $p < 0.05$

@ Significantly different from ICV-STZ group at $p < 0.05$

Significantly different from Antia (25 mg/kg) at $p < 0.05$

\$ Significantly different from Antia (50 mg/kg) at $p < 0.05$

Figure 6: Effect of Antia on protein expression in the hippocampi of ICV-STZ injected mice for (A) phosphorylated STAT and JAK, (B) GSK3 β and IKB α , (C) mTOR and p-AKT, and (D) COX-2.

* Significantly different from normal group at $p < 0.05$

@ Significantly different from ICV-STZ group at $p < 0.05$

Significantly different from Antia (25 mg/kg) at $p < 0.05$

\$ Significantly different from Antia (50 mg/kg) at $p < 0.05$

Figure 1

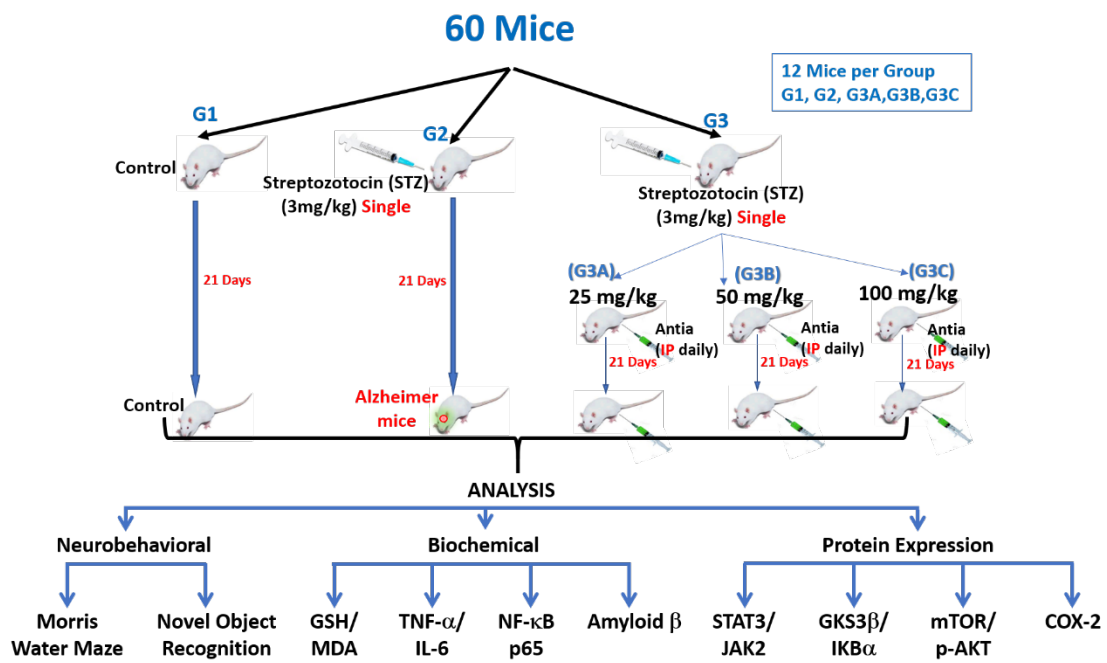


Figure 2A

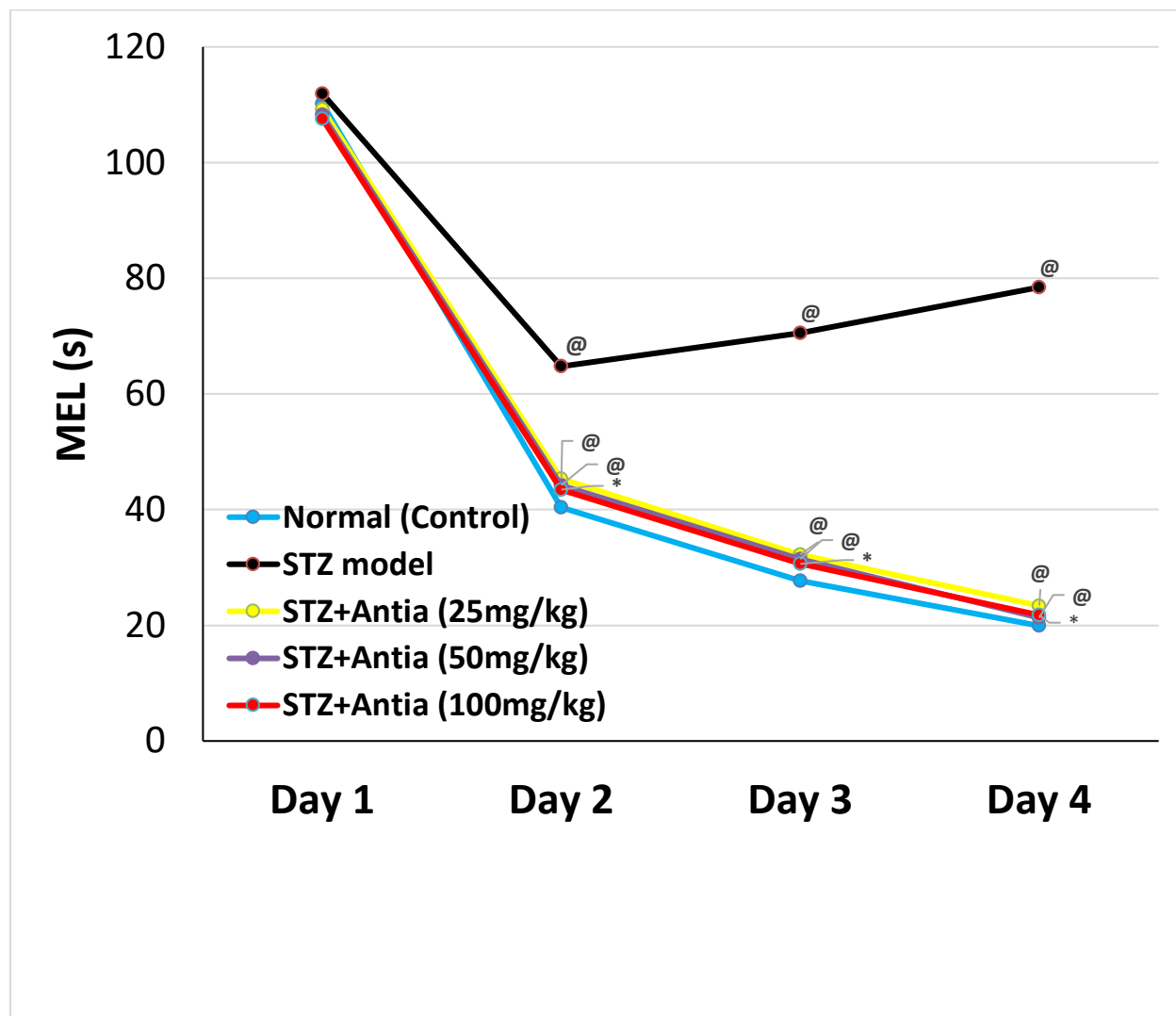


Figure 2B

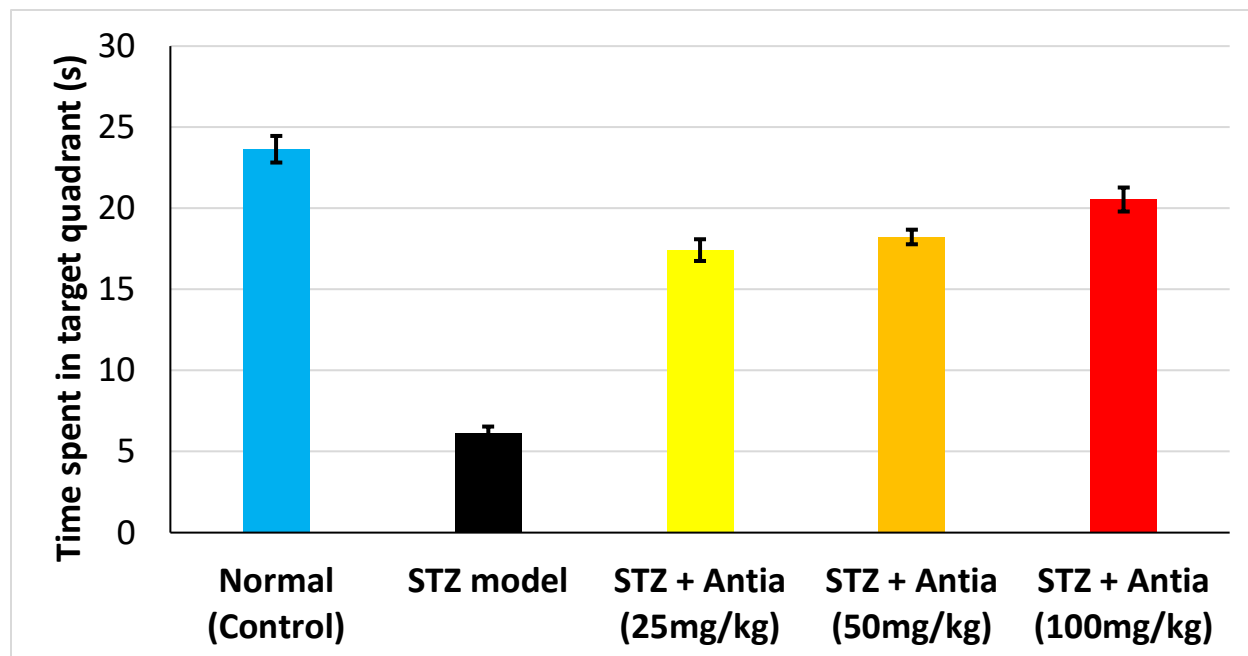


Figure 2C

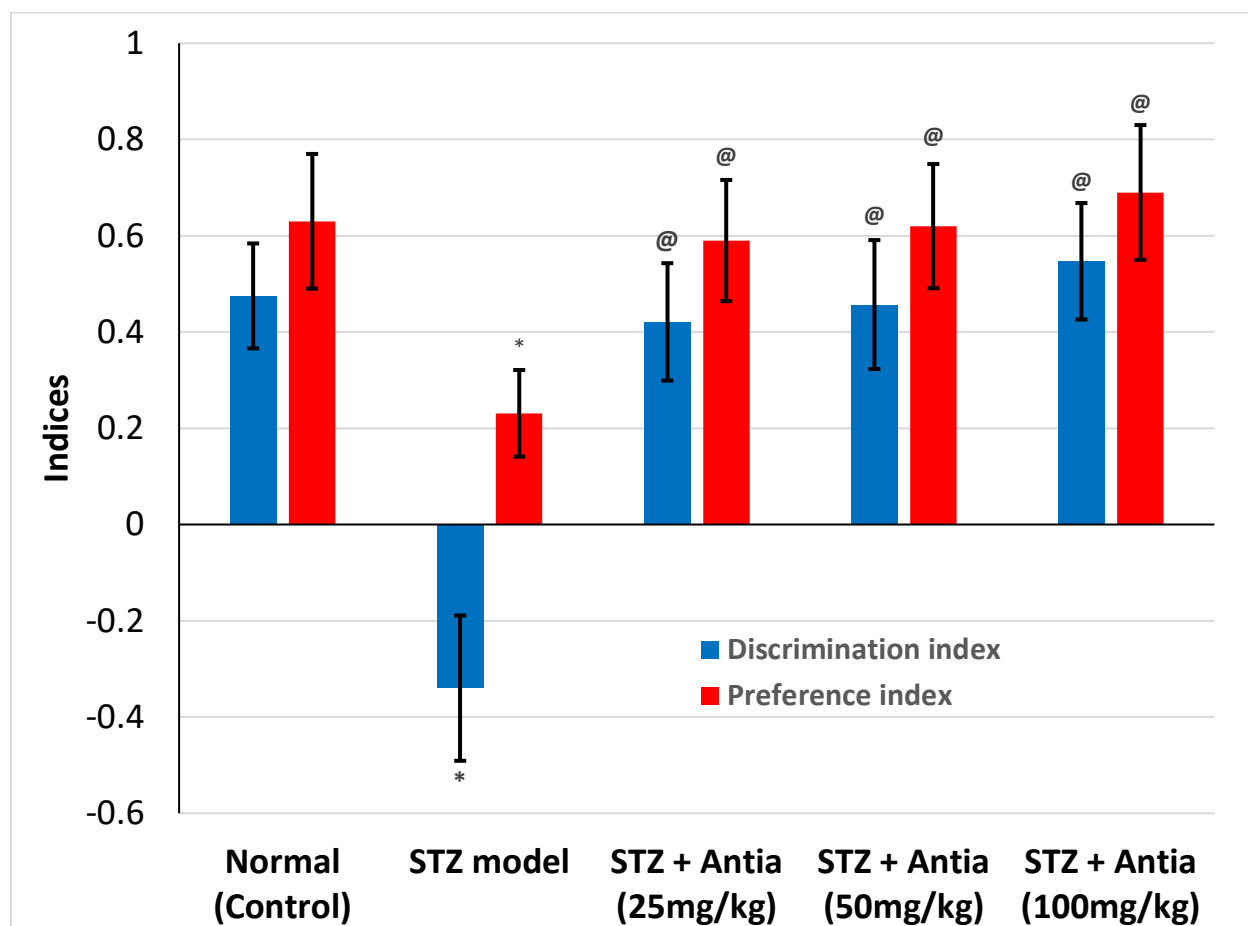


Figure 3A

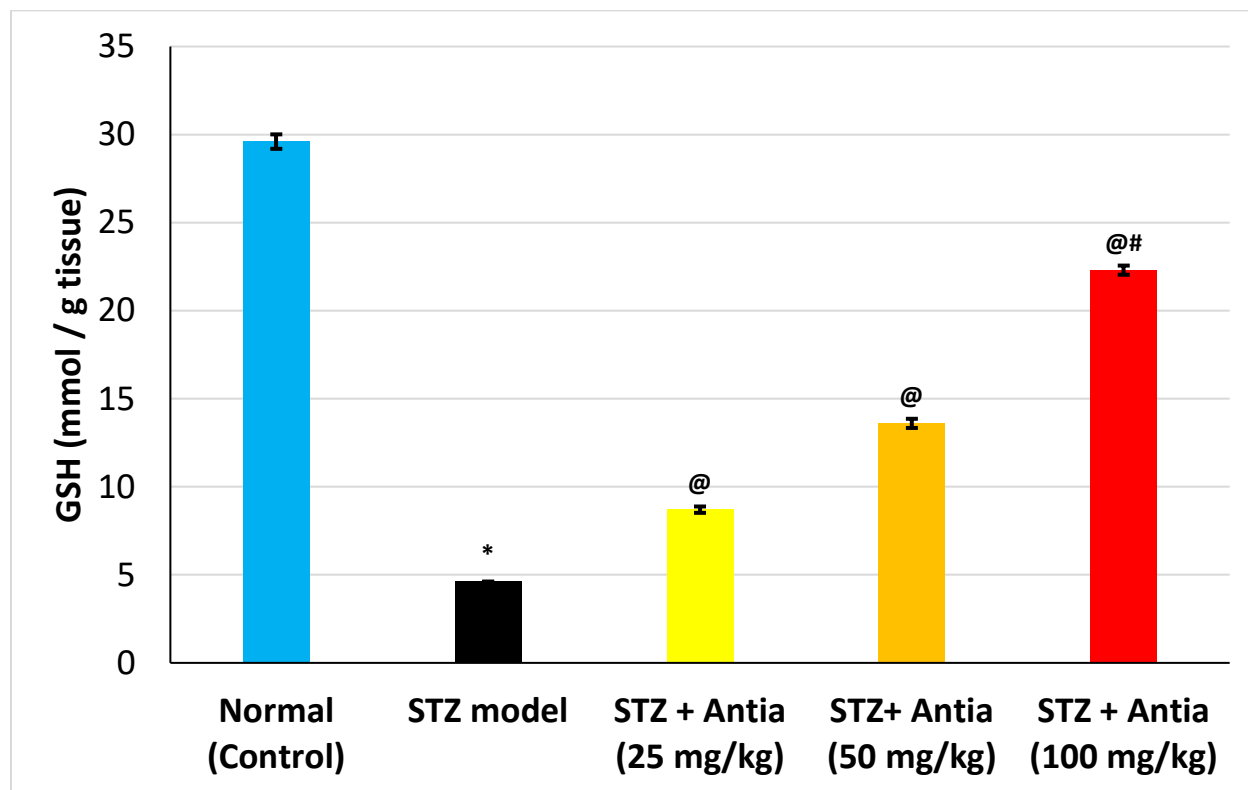


Figure 3B

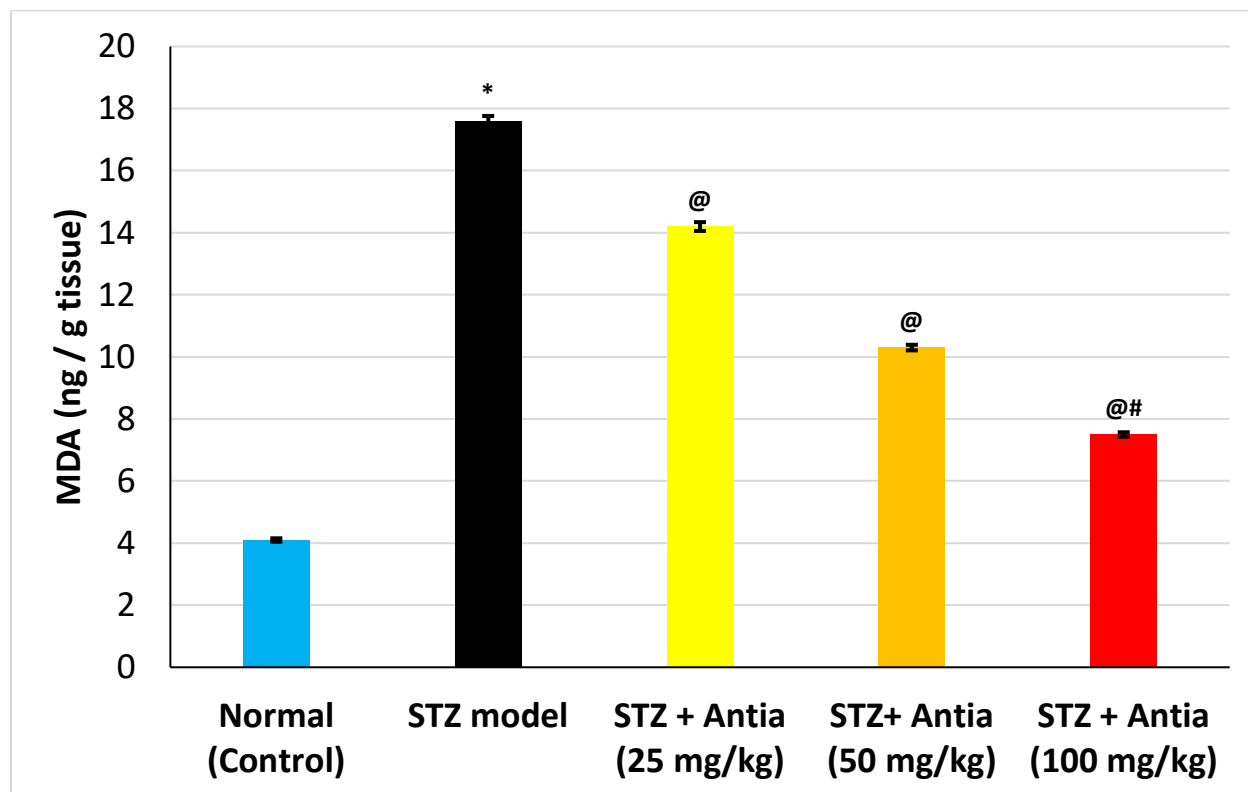


Figure 4

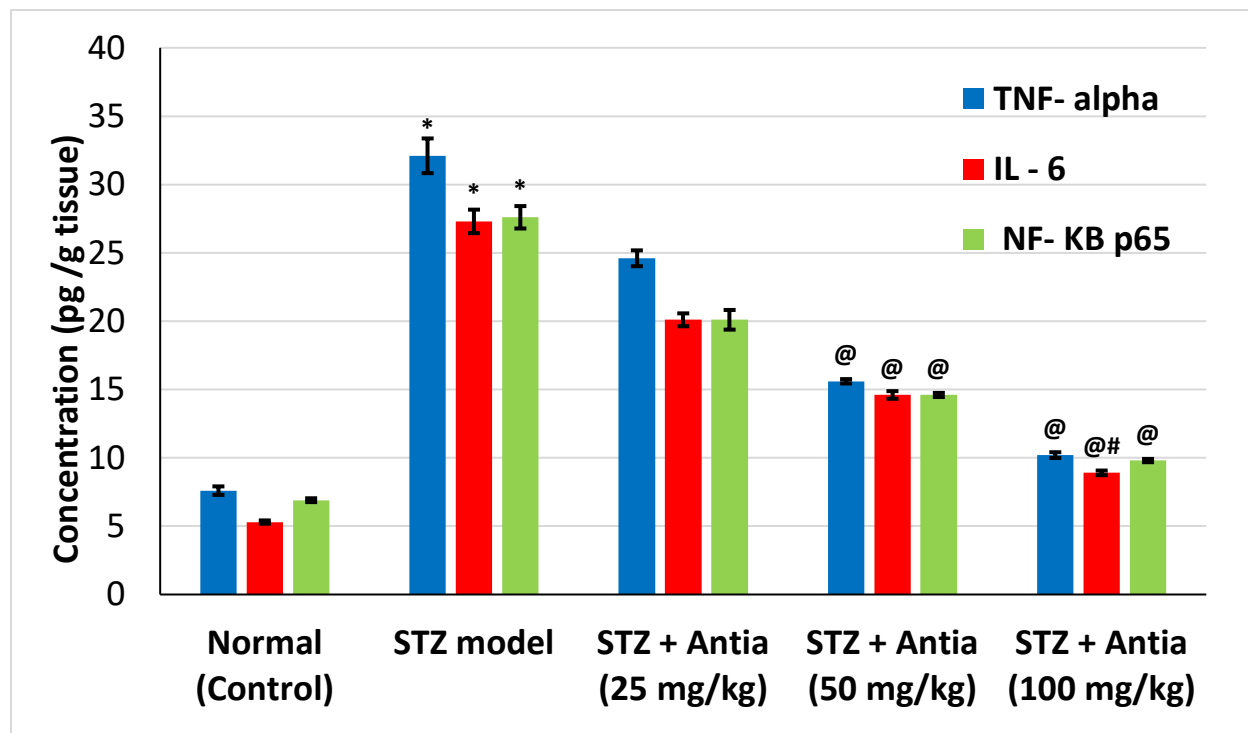


Figure 5

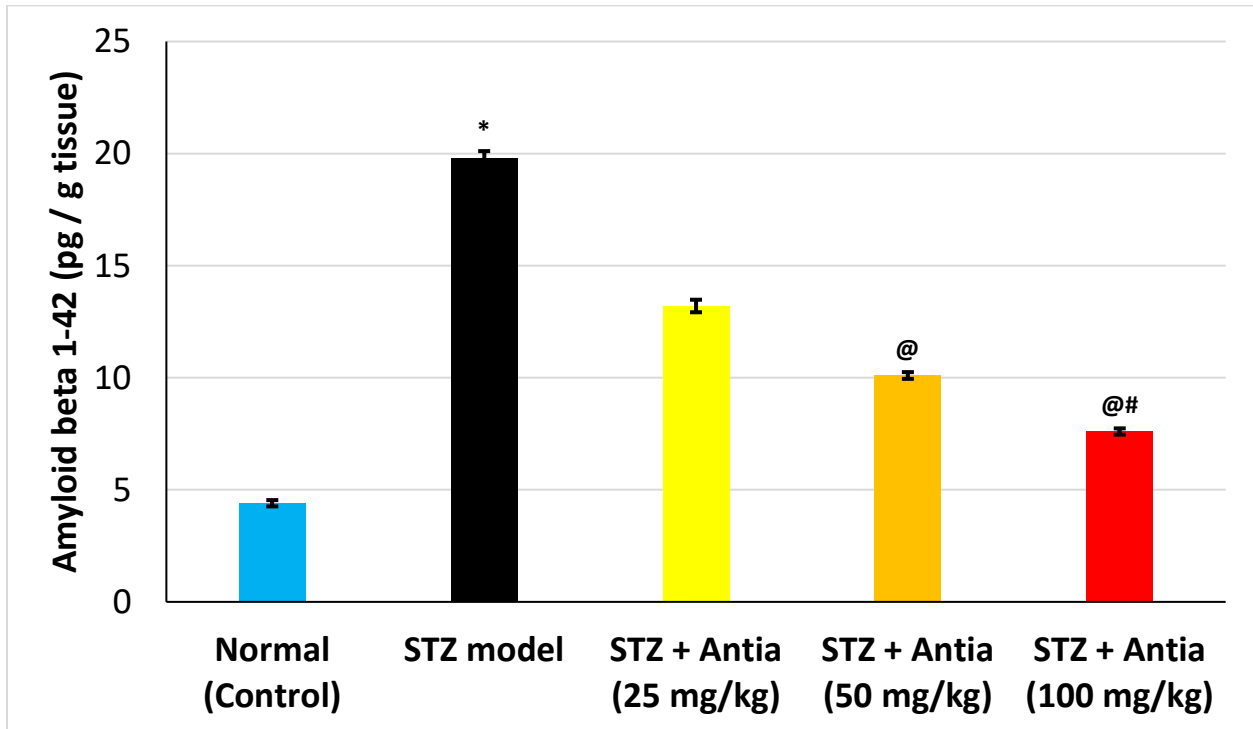
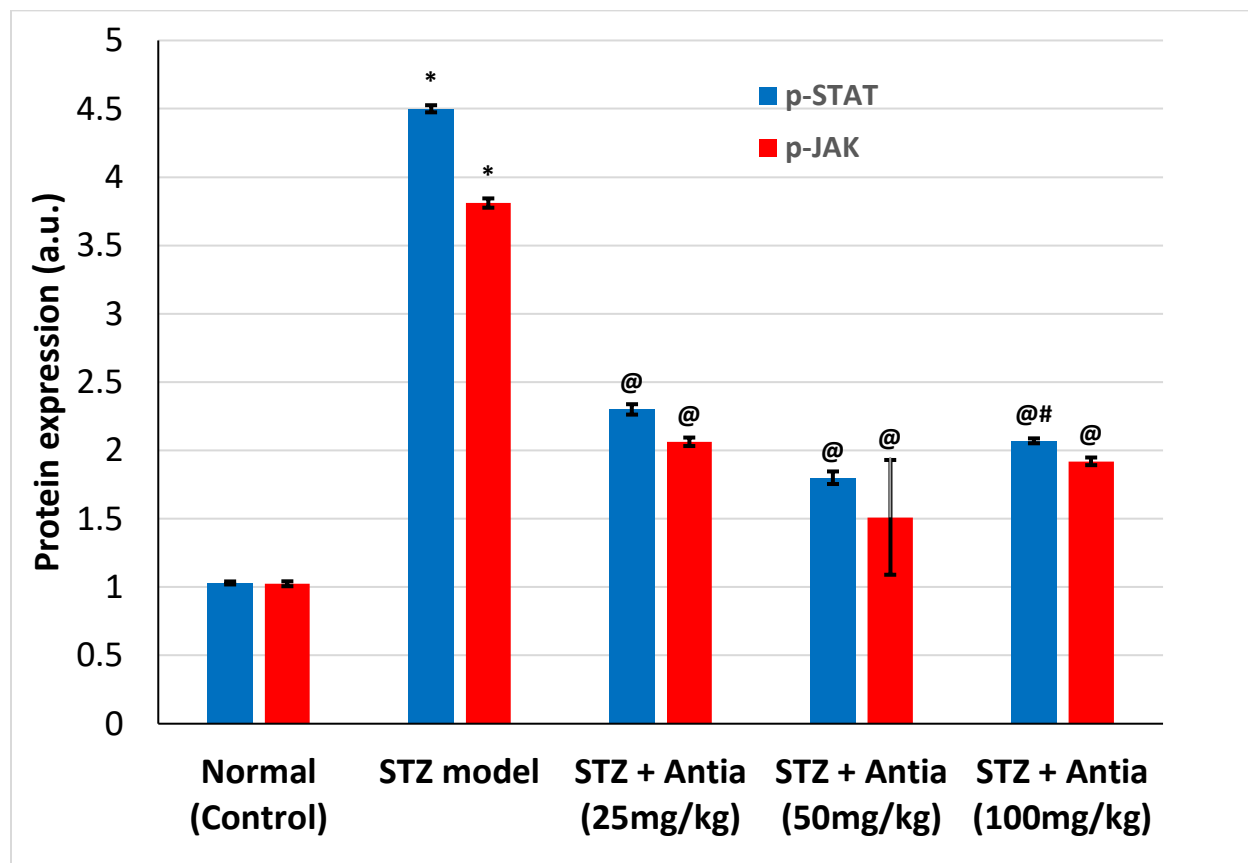


Figure 6A



p-STAT

p-JAK

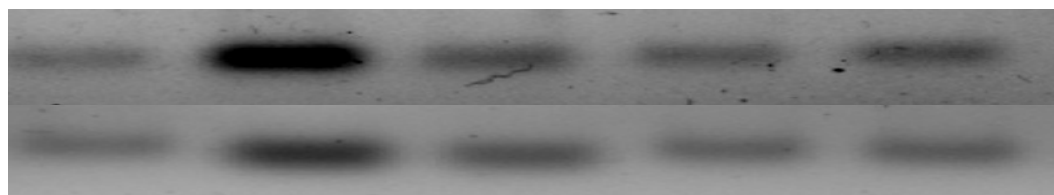


Figure 6B

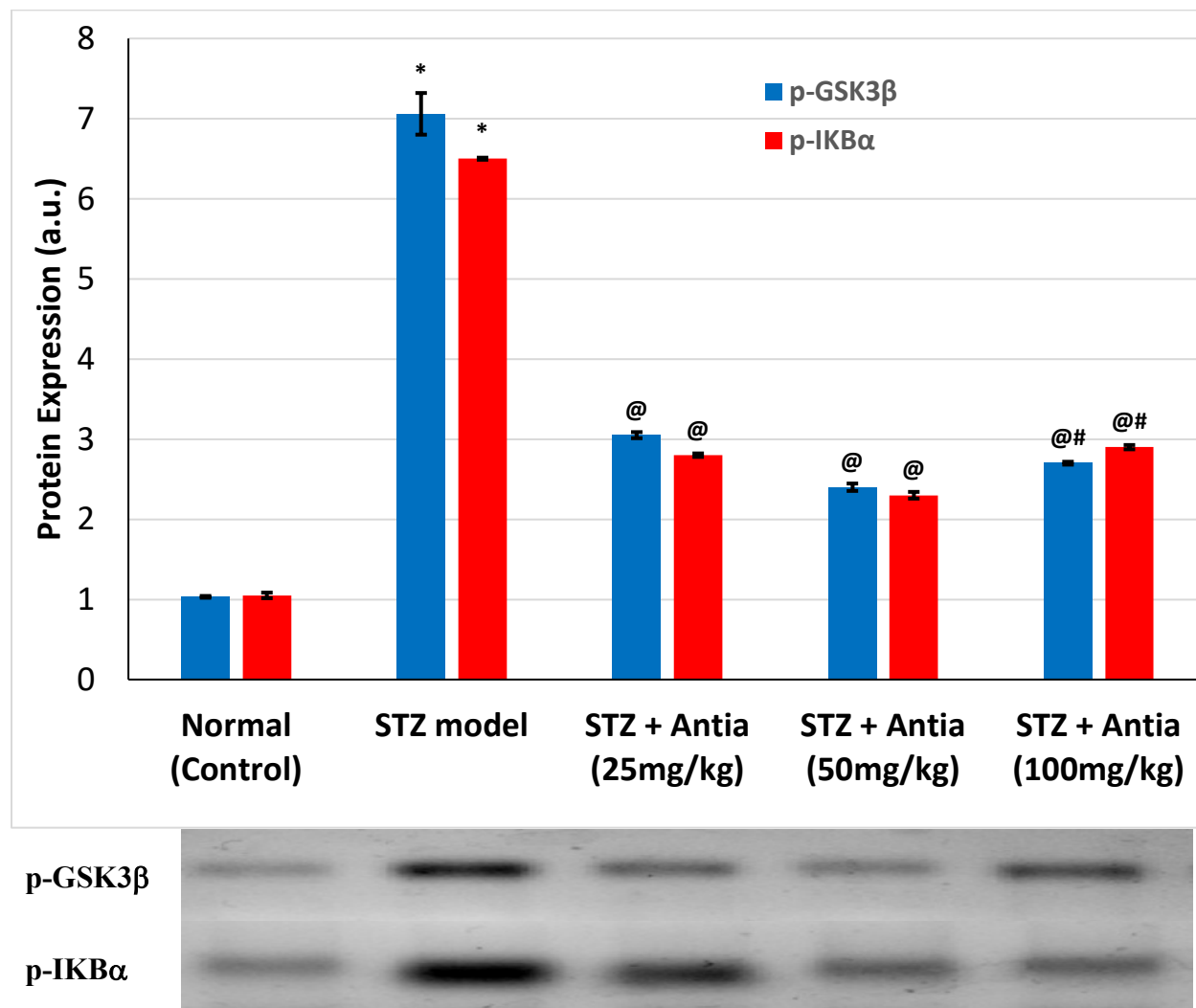
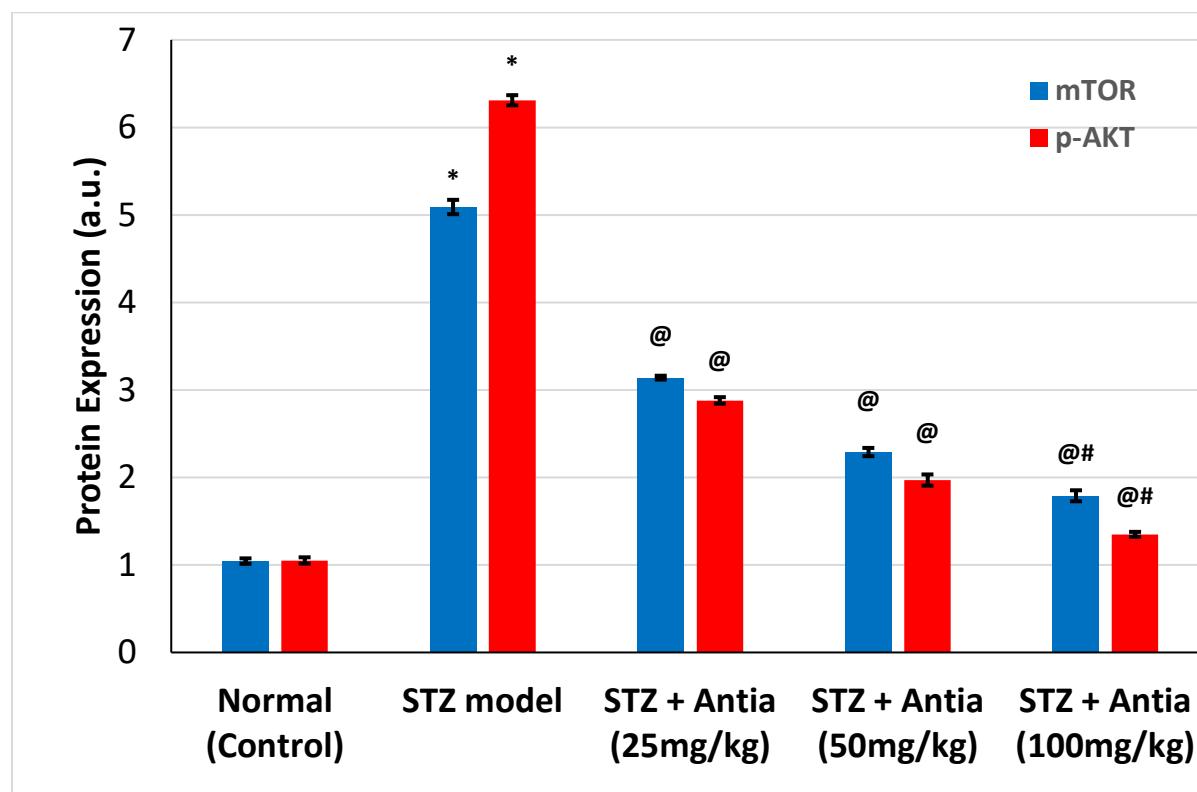


Figure 6C



mTOR

p-AKT

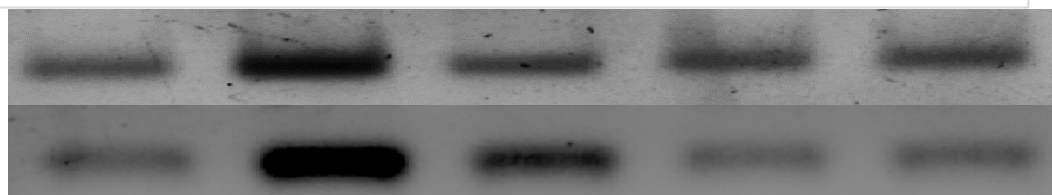


Figure 6D

